EUKARYOTIC CELL, Sept. 2009, p. 1397–1406 Vol. 8, No. 9
1535-9778/09/$08.00+0 doi:10.1128/EC.00378-08


# DYF-1 Is Required for Assembly of the Axoneme in *Tetrahymena thermophila*▽†

Drashti Dave, Dorota Wloga, Neeraj Sharma,‡ and Jacek Gaertig*

*Department of Cellular Biology, University of Georgia, Athens, Georgia 30602*

Received 1 December 2008/Accepted 24 June 2009

**In most cilia, the axoneme can be subdivided into three segments: proximal (the transition zone), middle (with outer doublet microtubules), and distal (with singlet extensions of outer doublet microtubules). How the functionally distinct segments of the axoneme are assembled and maintained is not well understood. DYF-1 is a highly conserved ciliary protein containing tetratricopeptide repeats. In *Caenorhabditis elegans*, DYF-1 is specifically needed for assembly of the distal segment (G. Ou, O. E. Blacque, J. J. Snow, M. R. Leroux, and J. M. Scholey. Nature. 436:583–587, 2005). We show that *Tetrahymena* cells lacking an ortholog of DYF-1, Dyf1p, can assemble only extremely short axoneme remnants that have structural defects of diverse natures, including the absence of central pair and outer doublet microtubules and incomplete or absent B tubules on the outer microtubules. Thus, in *Tetrahymena*, DYF-1 is needed for either assembly or stability of the entire axoneme. Our observations support the conserved function for DYF-1 in axoneme assembly or stability but also show that the consequences of loss of DYF-1 for axoneme segments are organism specific.**

Cilia are microtubule-rich cellular extensions that arise from basal bodies near the surfaces of most eukaryotic cell types. Defective cilia cause a wide variety of diseases, including polycystic kidney disease, primary ciliary dyskinesia, and retinal degeneration (3). A typical motile cilium has a microtubule-based framework, the axoneme, which contains nine outer (mostly doublet) microtubules and two central (singlet) microtubules. In most cilia, the axoneme can be subdivided into three segments: proximal (transition zone), middle (containing outer doublet microtubules), and distal (containing singlet extensions of peripheral microtubules). The outer doublet microtubules of the middle segment have a complete tubule A made of 13 protofilaments and an incomplete tubule B made of 11 protofilaments that is fused to the wall of the A tubule (36, 57). The outer microtubules in the distal segment lack the B tubule (32, 49). The distal segment also lacks dynein arms and radial spokes, and its microtubules are terminated by caps that are associated with the plasma membranes at the tips of cilia (11, 50). The distal segments are characterized by a high level of microtubule turnover, which could play a role in the regulation of the length of cilia (31).

The mechanisms that establish the segmental subdivision of the axoneme are not well understood. Studies of *Caenorhabditis elegans* indicate that the distal segment is assembled using a mechanism that differs from the one utilized in the middle and proximal segments (54). In most cell types, ciliogenesis is dependent on the intraflagellar transport (IFT) pathway, a bidirectional motility of protein aggregates, known as IFT particles, that occurs along outer microtubules (10, 28, 29, 42). IFT particles are believed to provide platforms for transport of axonemal precursors (23, 44). The anterograde component of IFT that delivers cargo from the cell body to the tips of cilia is carried out by kinesin-2 motors (28, 63), whereas the cytoplasmic dynein DHC1b is responsible for the retrograde IFT (41, 43, 53). Importantly, in the well-studied amphid cilia of *C. elegans*, two distinct kinesin-2 complexes are involved in the anterograde IFT and differ in movement velocity: the "slow" heterotrimeric kinesin-II and the "fast" homodimeric OSM-3 kinesin (54). While kinesin-II and OSM-3 work redundantly to assemble the middle segment, OSM-3 alone functions in the assembly of the distal segment (39, 56).

In *C. elegans*, DYF-1 is specifically required for assembly of the distal segment (39). In the DYF-1 mutant, the rate of IFT in the remaining middle segment is reduced to the level of the slow kinesin-II, suggesting that the Osm3 complex is nonfunctional and that kinesin-II functions alone in the middle segment. Thus, DYF-1 could either activate OSM-3 kinesin or dock OSM-3 to IFT particles (14, 39).

However, a recent study of zebrafish has led to a different model for DYF-1 function. Zebrafish embryos that are homozygous for a loss of function of fleer, an ortholog of DYF-1, have shortened olfactory and pronephric cilia and ultrastructural defects in the axonemes. In the middle segment, the *fleer* axonemes have B tubules that are disconnected from the A tubule, indicating that DYF-1 functions in the middle segment and could play a role in the stability of doublet microtubules (40). Earlier, a similar mutant phenotype was reported in *Tetrahymena* for a mutation in the C-terminal tail domain of β-tubulin, at the glutamic acid residues that are used by post-translational polymodifications (glycylation and glutamylation) (47). Glycylation (46) and glutamylation (12) are conserved polymeric posttranslational modifications that affect tubulin and are highly enriched on microtubules of axonemes and centrioles (reviewed in reference 20). Other studies have indicated that tubulin glutamylation contributes to the assembly and stability of axonemes and centrioles (4, 8). The *fleer* mu-

* Corresponding author. Mailing address: Department of Cellular Biology, University of Georgia, Athens, GA 30602. Phone: (706) 542-3409. Fax: (706) 542-4271. E-mail: jgaertig@cb.uga.edu.

† Supplemental material for this article may be found at http://ec.asm.org/.

‡ Present address: Department of Cell Biology, University of Alabama at Birmingham, Birmingham, AL 35294.

▽ Published ahead of print on 6 July 2009.

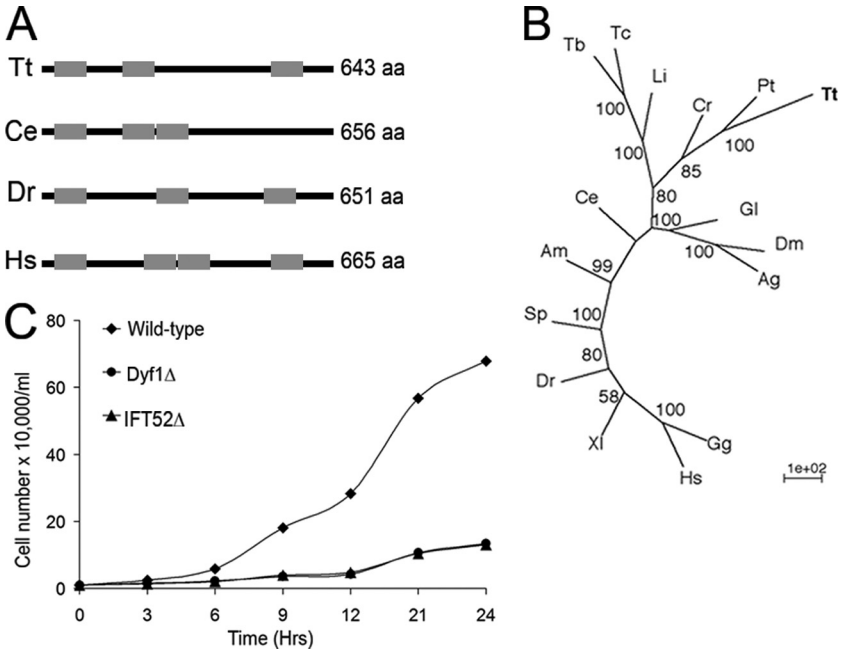


FIG. 1. *Tetrahymena* has a DYF-1 ortholog. (A) A schematic representation of DYF-1 protein sequences with TPR domains marked by gray boxes. aa, amino acids. (B) An unrooted phylogenetic tree of DYF-1 proteins. The tree was calculated by a neighbor-joining method. The nodes at branches indicate bootstrap values of >50%. Tt, *T. thermophila* (TTHERM_00313720); Pt, *P. tetraurelia* (XP_001424610.1); Cr, *C. reinhardtii* (XP_001692406.1); Li, *Leishmania infantum* (XP_001466521.1); Tb, *Trypanosoma brucei* (XP_844139.1); Tc, *Trypanosoma cruzi* (XP_818837.1); Gl, *Giardia lamblia* (XP_001706451.1); Dm, *Drosophila melanogaster* (CG5142-PB); Ag, *Anopheles gambiae* (XP_312036.2); Ce, *C. elegans* (F54C1.5a); Am, *Apis mellifera* (XP_397369.2); Sp, *Strongylocentrotus purpuratus* (XP_794254.2); Dr, *Danio rerio* (NP_001098119.2); Xl, *Xenopus laevis*; Hs, *Homo sapiens* (NP_689730.2); Gg, *Gallus gallus* (XP_426574.2). (C) Growth curves for DYF1Δ and IFT52Δ strains grown at 30°C in MEPP medium.

tant zebrafish cilia have reduced levels of glutamylated tubulin (40). Pathak and colleagues proposed that the primary role of DYF-1/fleer is to serve as an IFT cargo adapter for a tubulin glutamic acid ligase (25) and that the effects of lack of function of DYF-1/fleer could be caused by deficiency in tubulin glutamylation in the axoneme (40). As an alternative hypothesis, the same authors proposed that DYF-1 is a structural component that stabilizes the doublet microtubules in the axoneme (40).

Here, we evaluate the significance of a DYF-1 ortholog, Dyf1p, in *Tetrahymena thermophila*. Unexpectedly, we found that *Tetrahymena* cells lacking Dyf1p either fail to assemble an axoneme or can assemble an axoneme remnant. While our observations revealed major differences in the significance of DYF-1 for segmental differentiation in diverse models, it is clear that DYF-1 is a conserved and critical component that is required for assembly of the axoneme.

## MATERIALS AND METHODS

**Strains and cultures.** *T. thermophila* strains were grown at 30°C with shaking in either SPP (22) or MEPP (38) medium with an antibiotic-antimycotic mixture (Invitrogen, Carlsbad, CA). Strains CU428 and CU522 were obtained from the *Tetrahymena* Stock Center (Cornell University, Ithaca, NY).

**Phylogenetic analysis.** The sequences of DYF-1 homologs were obtained from the NCBI databases. Gene accession numbers are listed in the legend to Fig. 1. The sequences were aligned with ClustalX 1.82 (26) and corrected manually in SEAVIEW (21). A neighbor-joining tree was calculated using the Phylip package (SEQBOOT, PROTDIST, NEIGHBOR, CONSENSE, and DRAWGRAM) (15).

**Disruption of DYF1.** The coding region of *DYF1* (TTHERM_00313720) was identified in the *Tetrahymena* Genome Database by BLAST searches using the *C. elegans* DYF-1 sequence. Using *Tetrahymena* genomic DNA as a template, two nonoverlapping fragments of *DYF1* were amplified using the following primer pairs: 5′-ATAGGGCCCGTTTAGAGATACCAGAATTT-3′ plus 5′-TTTCCCGGGCT TGATTGGCTTCATTTTTT-3′and 5′-CCCACTAGTGCGTTTTGATTCTTT TTTG G-3′ plus 5′-TTTGCGGCCGCGGTATCAGTGTTAATCTTTT-3′.

Using restriction site sequences that were incorporated near the 5′ ends of the above-mentioned primers, the two fragments were subcloned into pTvec-Neo3 (51) so that the *neo3* gene was positioned in an opposite transcriptional orientation. The targeting fragments were designed to flank the first four exons (~1.6 kb) of *DYF1*. The targeting fragment was separated from the rest of the plasmid using ApaI and NotI. CU428 *Tetrahymena* cells were grown to $2 \times 10^5$ cells/ml and were starved at 30°C for 20 h in 10 mM Tris-HCl buffer, pH 7.5, and subjected to macronuclear biolistic transformation (9). The bombarded cells were incubated at 30°C for 2 h in SPP medium with 2 μg/ml $CdCl_2$, followed by selection in SPP medium with 100 μg/ml paromomycin and 2 μg/ml $CdCl_2$ at 30°C for 3 days. Several transformant clones were phenotypically sorted for a complete elimination of wild-type copies of *DYF1* by growing them under increasing selective pressure from paromomycin (up to 500 μg/ml) and 1 μg/ml $CdCl_2$ for 14 days. Single-cell isolations were made in drops of drug-free MEPP medium. Immotile cells appeared in 31% of the drops ($n = 96$). The immotile cells were reisolated twice. Upon prolonged growth (20 generations) in a drug-free medium, no reversion to a motile phenotype was observed, indicating that all native copies of *DYF1* were lost due to phenotypic assortment.

The *Tetrahymena* gene (TTHERM_00134890) encoding a protein orthologous to PF20 of *Chlamydomonas reinhardtii* (55) was eliminated from the macronucleus using a similar strategy. The following primers were used to amplify targeting fragments for PF20 that were subcloned on the sides of the *neo2* cassette: 5′-TTATA GAGCTCGCAACGGGTTACAAGACT-3′, 5′-ATATTGGATCCTGGCTTTTT ATCTTCCTTAG-3′, 5′-TAATTGGATCCCGAAGATAAAGTAGAAGACG-3′, and 5′-AATTACTCGAGATATCATTTATCCTTGCTTCTA-3′.

**Phenotypic studies.** To measure the rate of phagocytosis, cells were fed with 0.2% India ink in SPP for 15 min at 30°C and fixed with 2% paraformaldehyde.

To measure the rate of cell locomotion, paths of moving cells were recorded using a Nikon TMS microscope and measured using NIH Image 1.62. To determine the growth rate, cells (at the initial concentration of $10^4$ cells/ml) were grown in 25 ml of MEPP at 30°C and counted every 3 h.

**GFP tagging of Dyf1p.** The predicted coding sequence of *DYF1* was amplified using primers 5′-AAAACGCGTCATGAAGCCAATCAAGTAGATT-3′ and 5′-TTTGGATCCTAATTTTATCAATTTCTTAACTTG-3′. The resulting fragment was digested using MluI and BamHI and ligated into pMTT1-GFP for N-terminal tagging with green fluorescent protein (GFP). The *DYF1* knockout cells were starved overnight in 10 mM Tris-HCl, pH 7.5, at room temperature and biolistically transformed as described above, suspended in MEPP medium with 1.5 μg/ml $CdCl_2$, and incubated at 30°C for 3 days. Transformant clones were identified based on the recovery of cell motility. As a negative control, a mock biolistic transformation was performed without plasmid DNA.

**Microscopy.** For immunofluorescence with 12G10 anti-α-tubulin monoclonal antibody (1:50 dilution) and SG polyclonal anti-tubulin antibodies (1:100), ~100 *Tetrahymena* cells were simultaneously fixed and permeabilized with 2% paraformaldehyde and 0.5% Triton X-100 in PHEM buffer (60 mM PIPES, 25 mM HEPES, 10 mM EGTA, 2 mM $MgCl_2$). For staining with ID5 monoclonal antibody (48), which in *Tetrahymena* is specific for polyglutamylated tubulin (66) (1:40 dilution), ~100 *Tetrahymena* cells were isolated on coverslips, permeabilized with 0.5% Triton X-100 in PHEM buffer for 45 s, and fixed with 2% paraformaldehyde in the same buffer. Cells fixed with either method were air dried at 30°C and processed for immunofluorescence labeling as described previously (18). The secondary antibody used was either goat anti-mouse- or goat anti-rabbit–fluorescein isothiocyanate conjugate (1:200; Zymed). For direct detection of GFP and testing the solubility of GFP fusion proteins, cells expressing either GFP-Dyf1p or IFT52p-GFP, or GFP alone, were prepared for microscopic observations using the following three methods (all fixations/permeabilizations were solutions based on the PHEM buffer): cells (~$1 \times 10^5$) were washed with 10 mM Tris, pH 7.5, and the pellet (i) was combined with 300 μl of 0.5% Triton X-100 and, after 3 min, washed with PHEM buffer (1 ml) and fixed with 2% paraformaldehyde (300 μl) for 30 min; (ii) was combined with 300 μl of 2% paraformaldehyde for 30 min; or (iii) was combined with 300 μl of 0.25% Triton X-100 and 1% paraformaldehyde for 30 min. All samples were washed with phosphate-buffered saline and observed as explained above. For transmission electron microscopy (TEM), cells were processed as described previously (27).

## RESULTS

**Loss of Dyf1p results in extreme truncation of cilia and severe axonemal defects.** Using the *C. elegans* protein sequence of DYF-1 (F54C1.5a), we searched gene predictions derived from the *Tetrahymena* macronuclear genome (13) available at the *Tetrahymena* Gene Database using pBLAST, and we identified a single gene, named *DYF1*, encoding a closely related protein (TTHERM_00313720). The predicted Dyf1p amino acid sequence is 43% identical to that of DYF-1 of *C. elegans*. Dyf1p is predicted to have three tetratricopeptide (TPR) domains that are located at positions similar to those in other DYF-1 proteins (Fig. 1A). Phylogenetic analyses showed that Dyf1p is most closely related to homologs of other protists, *Paramecium tetraurelia* (GSPATT00028247001) and *C. reinhardtii* (FAP259) (Fig. 1B).

Next, we eliminated all expressed copies of *DYF1* by DNA homologous recombination. Ciliates have two functionally distinct nuclei, the micronucleus and the macronucleus. Only the macronuclear genes contribute to the phenotype in vegetatively growing cells. There are about 45 copies of each protein-coding gene in the $G_1$ macronucleus (reviewed in reference 61). We constructed *Tetrahymena* strains with a macronuclear knockout of *DYF1* via DNA homologous recombination, using a fragment of *DYF1* interrupted by *neo3* (51) (see Fig. S1 in the supplemental material) and eliminated all macronuclear copies of *DYF1* by phenotypic assortment under drug selection that favored retention of the *neo3*-disrupted alleles (see Materials and Methods). After 2 weeks of selective growth, single cells were isolated in drug-free medium. Among the isolates, we detected clones in which all or nearly all cells were paralyzed. Recloning of the motility-deficient cells established phenotypically stable populations of paralyzed cells that also displayed frequent arrests in cytokinesis and become multinucleated (data not shown). The cytokinesis failure was consistent with loss of ciliary motility (6, 7, 59, 64). These observations indicated that phenotypic assortment under drug selection had produced cells lacking macronuclear copies of *DYF*. Importantly, we rescued the motility of paralyzed DYF1Δ cells by biolistic bombardment with a transgene encoding GFP-Dyf1p inserted into another nonessential locus (see below). Thus, we conclude that Dyf1p is required for cell motility.

A DYF1Δ population grew with a generation time that was twice as long as that of the wild type (Fig. 1C) at a rate similar to the rate displayed by a strain lacking Ift52p, an IFT complex B protein, in which cilia fail to assemble (6). Video recordings of live cells showed that DYF1Δ cells were completely paralyzed (Fig. 2A to C). In addition to locomotory functions, *Tetrahymena* cells use oral cilia for phagocytosis (38). Wild-type cells fed with India ink had an average of ~6.8 ink-filled food vacuoles per cell after 15 min of incubation in medium with ink ($n = 39$). Ink-filled vacuoles were not observed in DYF1Δ cells, even after 30 min ($n = 40$) (data not shown). Thus, Dyf1p is needed for the functions of both locomotory and oral cilia.

Immunofluorescence of DYF1Δ cells with anti-tubulin antibodies showed that extremely short axonemes were present (Fig. 2D and E), which resembled those observed in IFT52Δ cells, which are deficient in anterograde IFT (Fig. 2F) (6) or kinesin-2 (7), except that many axoneme stubs appeared slightly longer in DYF1Δ cells (Fig. 2E and F).

TEM showed that basal bodies in DYF1Δ cells had a wild-type appearance (Fig. 3; results not shown for cross sections). In the longitudinal sections, most basal bodies (82%) had at least a partially assembled axoneme (Fig. 3B to D and Table 1). Among the basal bodies lacking an axoneme, most had the central granule (the structure from which the central microtubules originate), but the corresponding portions of outer doublet microtubules were often either partly or completely missing (Fig. 3E and F). Thus, the lack of Dyf1p affects the organization of microtubules within the transition zone. Many basal bodies lacking an axoneme were associated with an apparent ciliary membrane outgrowth (Fig. 3E and F and 4I and J and Table 1). In contrast, in IFT52Δ cells, ~80% of basal bodies entirely lacked an axoneme and the naked basal bodies lacked membrane outgrowths (Table 1) (6). In the DYF1Δ cells, the axoneme, if present, could assemble to various extents (Fig. 3B to D). Moreover, nearly all axoneme remnants of DYF1Δ cells had an abnormal organization (Table 2). Frequently, DYF1Δ axoneme cross sections lacked central pair microtubules (Fig. 4C to H) or one or more outer microtubules (Fig. 4E). Many DYF1Δ axoneme cross sections contained a mixture of outer doublets and singlets, indicating instability or failure to assemble the B tubule (Fig. 4B, D, and F), or had partially truncated or opened B tubules (Fig. 4G and H). Thus, DYF1Δ cells can assemble only extremely short and highly disorganized axonemes.

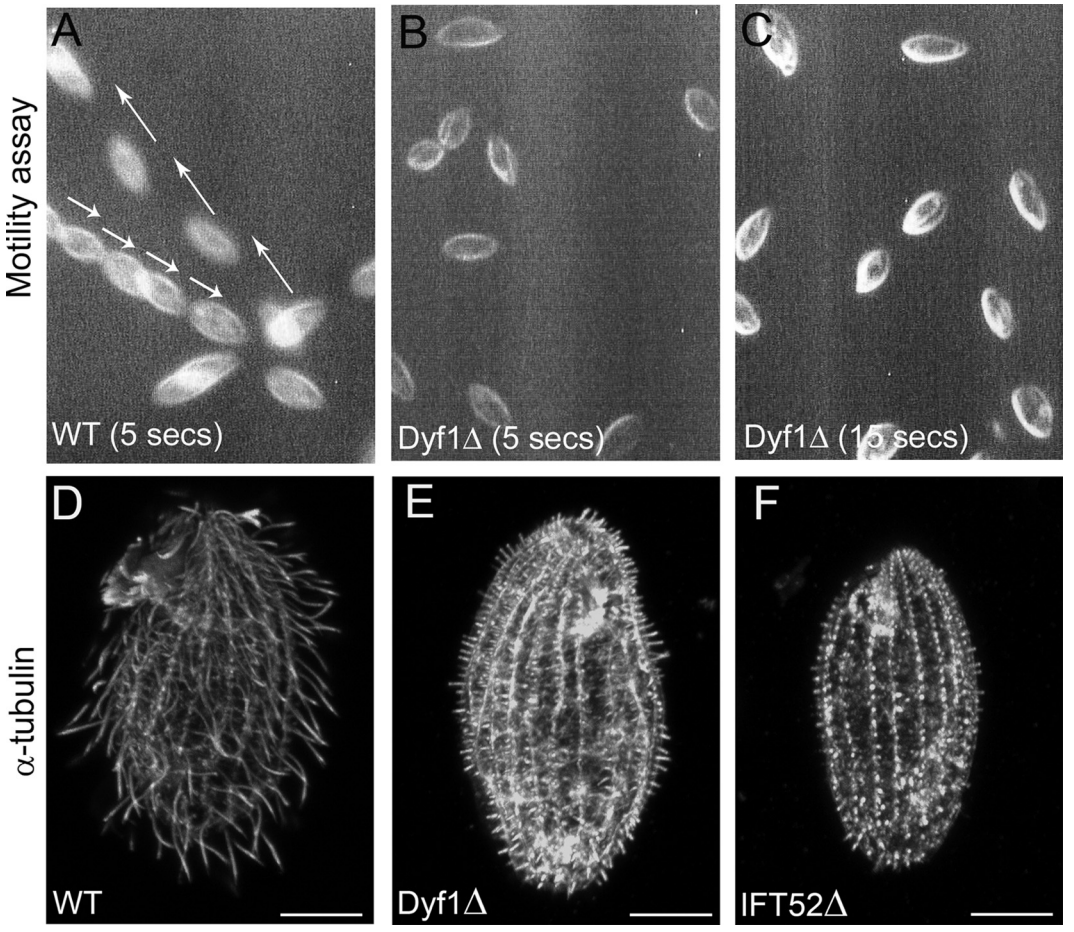


FIG. 2. Dyf1p is required for axoneme assembly. (A to C) Video images of live wild-type (WT) cells recorded for 5 s (A) and DYF1Δ recorded for 5 s (B) and 15 s (C). The paths of motile wild-type cells are marked with arrows. Note that DYF1Δ cells do not show motility even over 15 s. (D to F) Wild-type (D), DYF1Δ (E), and IFT52Δ (F) cells stained with anti-tubulin antibodies. Bars, 10 μm.

**Dyf1p localizes to the basal bodies and cilia.** To test whether the ciliary defects observed in DYF1Δ cells are caused by the loss of Dyf1p, we attempted to rescue the DYF1Δ cells with a transgene encoding GFP-Dyf1p that was targeted to a nonessential *BTU1* locus (19). Among the DYF1Δ cells bombarded with a GFP-DYF1 transgene, motile cells appeared at a frequency of 0.007%, while no motile cells were seen among the mock-transformed cells ($n = 10^7$). Rescued GFP-Dyf1p cells were motile and had a wild-type morphology (Fig. 5A to A″). GFP-Dyf1p localized to basal bodies and along axonemes, which resembled the localization of GFP-Ift52p (6). GFP alone that was expressed in the same locus and under the same promoter did not localize to cilia or basal bodies (Fig. 5B to B″). The GFP-Dyf1p signal was lost almost completely when cells were extracted with a detergent prior to fixation (Fig. 6 to A″). A similar observation was made for cells expressing GFP-IFT52p (Fig. 6B to B″). These observations indicate that Dyf1p is not stably associated with the axoneme and most likely is a component of the ciliary matrix. Strong overproduction of GFP-Dyf1p had no obvious effect on the length of cilia or cell motility (results not shown).

**Residual axonemes in the *DYF1* knockout cells have hyperglutamylated microtubules.** A study of zebrafish showed that DYF-1/*fleer* mutants have short cilia that have reduced levels of tubulin glutamylation (40). We evaluated DYF1Δ cells by immunofluorescence with ID5, a monoclonal antibody (48) that in *Tetrahymena* is specific for polyglutamylated tubulin (66). Unexpectedly, the levels of tubulin polyglutamylation were increased in the axoneme remnants of DYF1Δ cells imaged side by side with wild-type axonemes (Fig. 5C). In wild-type cells, ID5 strongly labeled basal bodies and weakly labeled axonemes (Fig. 5C). However, in the DYF1Δ mutants, the signals of ID5 are equally strong in the basal body and in the axoneme remnant (Fig. 5C). In wild-type cells, short cilia that are in the course of assembly have increased levels of tubulin glutamylation compared to full-length mature cilia (52). We compared wild-type cells undergoing cilial regeneration (after deciliation) with DYF1Δ cells side by side (Fig. 5D). It appears that the levels of tubulin polyglutamylation in axoneme stubs in DYF1Δ cells are higher even than in assembling wild-type axonemes. Thus, the DYF1Δ axoneme remnants have hyperglutamylated microtubules.

Interestingly, the axoneme stubs in IFT52Δ cells also have elevated levels of tubulin glutamylation (Fig. 5E). Thus, tubulin hyperglutamylation could be generally associated with failed axoneme assembly. However, it is known that some

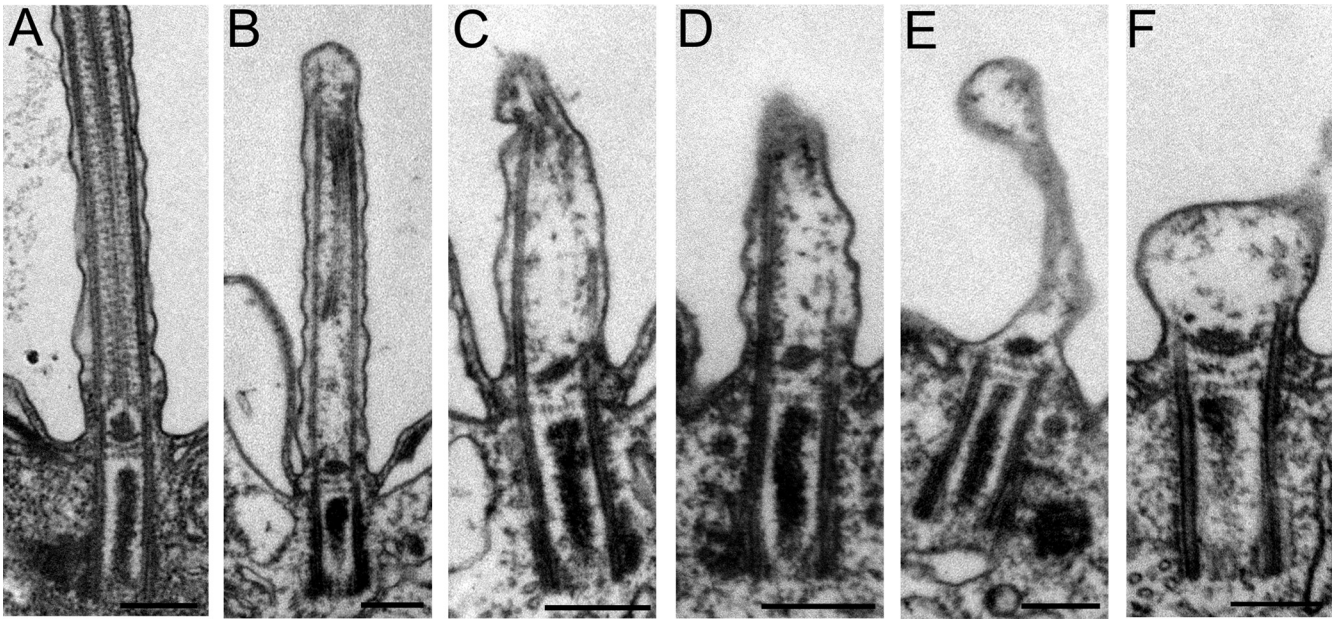


FIG. 3. Loss of function of *DYF1* results in shortened, disorganized, or missing axonemes. Shown are longitudinal TEM sections of wild-type cilia (A) and DYF1Δ cilia (B to F). Bars, 0.2 μm.

posttranslational modifications of tubulin accumulate on long-lived microtubules (reviewed in reference 62). Thus, an alternative explanation is that the longer cell cycle in cells lacking functional cilia (Fig. 1C) is associated with accumulation of posttranslationally modified microtubules. However, antibodies specific for monoglycylation (TAP952) and polyglycylation (AXO49) (5) showed no obvious differences in the levels of glycylated tubulin isoforms between wild-type and DYF1Δ or IFT52Δ axonemes and basal bodies (data not shown). To explore further whether a longer cell cycle is associated with increased tubulin glutamylation in axonemes, we created a knockout strain lacking a *Tetrahymena* ortholog of PF20 (TTHERM_00134890), a protein required for stability of the central pair in *C. reinhardtii* (55). PF20Δ cells were paralyzed and grew slowly, with a generation time similar to those of DYF1Δ and IFT52Δ cells (see Fig. S2B in the supplemental material). PF20Δ cells assembled normal-length axonemes. TEM showed a mixture of nine plus two and nine plus zero axoneme cross sections, indicating a partial defect in the formation or stability of central microtubules (our unpublished data). A side-by-side labeling of PF20Δ and wild-type cells showed only a slight increase in the levels of tubulin glutamylation in the basal bodies and axonemes of PF20Δ cells (see Fig. S2A to A3 in the supplemental material). However, unlike in DYF1Δ and IFT52Δ cells, the axoneme in PF20Δ cells maintained a lower level of glutamylation than the adjacent basal body (see Fig. S2A to A3 in the supplemental material). We conclude that hyperglutamylation of residual axonemes in IFT52Δ and DYF1Δ cells cannot be explained solely by an increased time of exposure to tubulin-modifying enzymes and that in *Tetrahymena*, tubulin hyperglutamylation could be associated with a severe failure of axonemal assembly.

TABLE 1. Quantification of TEM images of longitudinal sections through basal bodies

| Strain | % of TEM images | | |
|---|---|---|---|
| | With an axoneme | With a membrane bubble | Naked basal body |
| DYF1Δ ($n$ = 28) | 82.1 | 10.7 | 8.7 |
| IFT52Δ ($n$ = 84) | 21.4 | 0 | 78.6 |
| Wild type ($n$ = 23) | 86.95 | 0 | 13.05[a] |

[a] Some basal bodies remain unciliated for most of the cell cycle in the wild type.

## DISCUSSION

Studies of *C. elegans* showed that the assembly of the distal segments of axonemes that contain only A tubules of outer microtubules requires the homodimeric OSM-3 kinesin motor and DYF-1. It has been proposed that DYF-1 activates OSM-3 or links IFT particles to OSM-3 (14, 39, 56). *Tetrahymena* has the distal portions of cilia with prominent singlet extensions (49, 58). Moreover, the genome of *Tetrahymena* encodes orthologs of motor subunits of OSM-3 kinesin-2, including Kin5p, a motor that localizes to cilia (2), and as we show here, *Tetrahymena* has a *DYF1* ortholog, Dyf1p. To our surprise, knocking out *DYF1* in *Tetrahymena* resulted in a complete or nearly complete loss of the axoneme, indicating that in *Tetrahymena*, DYF-1 is required for either the assembly or stability of all axoneme segments. Studies of zebrafish and *Trypanosoma* support our observations, indicating a broader role for DYF-1 in axoneme assembly or stability. Cilia in the zebrafish DYF-1/*fleer* mutant embryos, in addition to reduced length, showed defects in the structure of the outer doublets in the middle segment (40). Consistently, in *Tetrahymena* cells lacking DYF-1, the B tubule is often either completely absent or

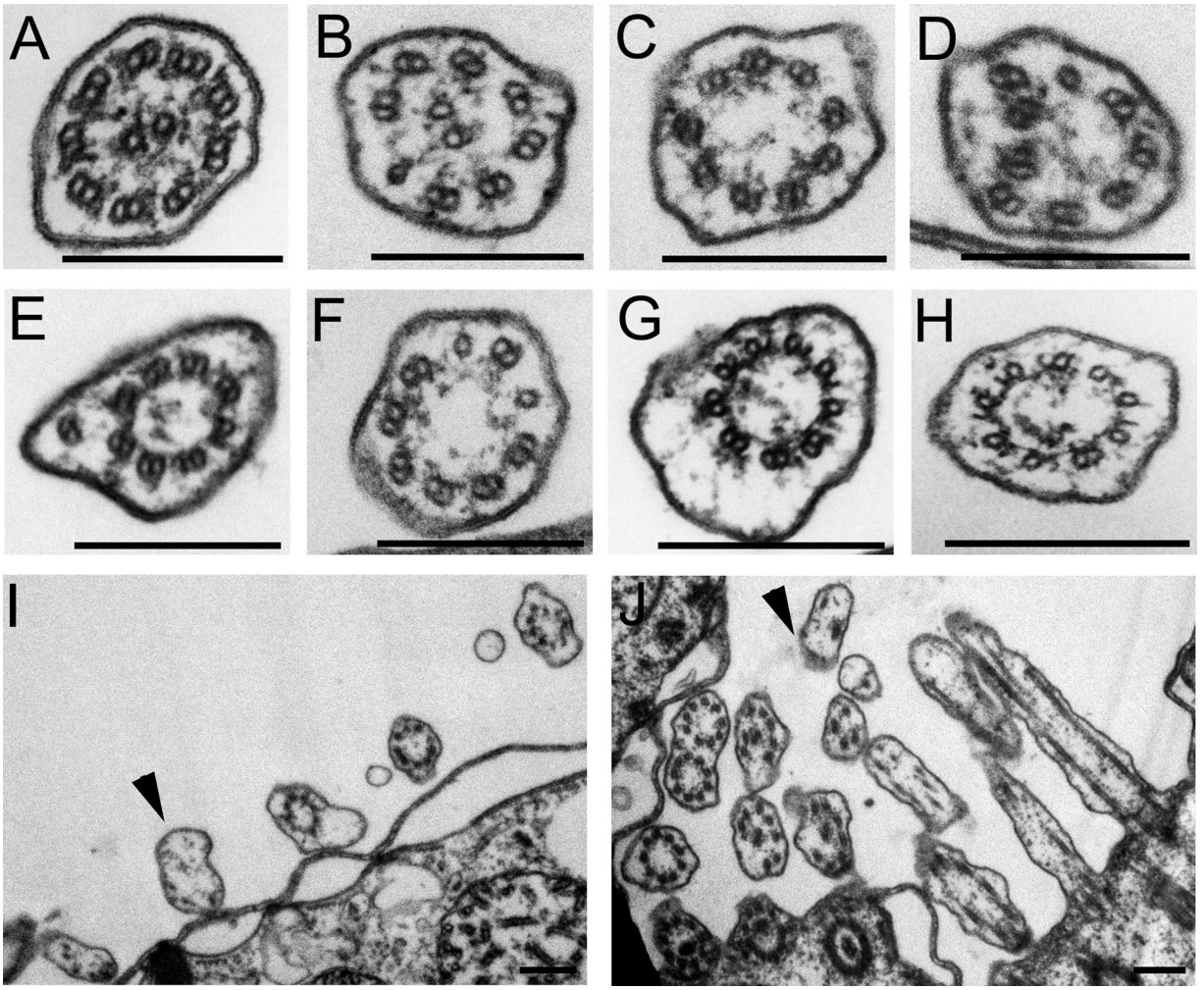


FIG. 4. Loss of function of *DYF1* severely disorganizes the axoneme. Shown are TEM cross sections of wild-type (A), DYF1Δ locomotory (B to I), and DYF1Δ oral (J) cilia. DYF1Δ locomotory cilia have a wide range of defects: missing central pair microtubules (C to J), incomplete B tubules (G and H), outer singlet microtubules (B, D, and F), and displaced outer doublet microtubules (D and E). (I and J) Portions of the DYF1Δ somatic cortex (I) and oral region (J). The arrowheads mark membrane outgrowths. Bars, 0.2 μm.

detached from the A tubule. Moreover, in cilia of *Tetrahymena* and in zebrafish deficient in DYF-1, central microtubules fail to assemble (see Fig. 7B in reference 40). Recently, RNA interference-based depletion of a DYF-1-related protein of *Trypanosoma* has led to loss of flagella, consistent with a role of DYF-1 for the entire axoneme (1).

TABLE 2. Frequencies of various structural defects on cross sections of non-oral DYF1Δ axonemes

| Axonemal organization | % in DYF1Δ ($n$ = 121) | % in wild type ($n$ = 167) |
|---|---|---|
| 9 + 2 (normal) | 6.6 | 97 |
| 9 + 0 | 19 | 0 |
| Missing outer doublets, central pair present | 20.6 | 0 |
| Outer singlets, central pair present | 11.6 | 3[a] |
| Outer doublets and singlets without a central pair | 22.3 | 0 |
| Outer doublets and singlets with a central pair | 1.7 | 0 |
| Membrane bubbles lacking an axoneme | 18.2 | 0 |

[a] This corresponds to the distal segments that have singlet outer tubules.

At first, the zebrafish data (40) and the *Trypanosoma* data (1) appear to contradict the *C. elegans* studies (14, 39) showing a specific requirement for DYF-1 for distal-segment assembly. However, it is possible that the different outcomes of DYF1 deficiencies in diverse models reflect structural and functional differences between the cilia in these models. In particular, cilia in *C. elegans* are unique due to their lack of motility, absence of central microtubules, and unusual arrangement of outer microtubules (24). However, it is possible that in *Tetrahymena*, zebrafish, and *Trypanosoma*, DYF-1 is also specifically involved in the assembly of the distal segment but that failure to develop the distal segment leads to a catastrophic lack of stability of the entire axoneme. For example, failure to assemble the distal segment could prevent the assembly of caps, structures that connect the ends of outer and central pair microtubules to the ciliary membrane (11). This hypothesis could be tested in the future, if a temperature-sensitive mutation in Dyf1p can be identified to destabilize the activity of

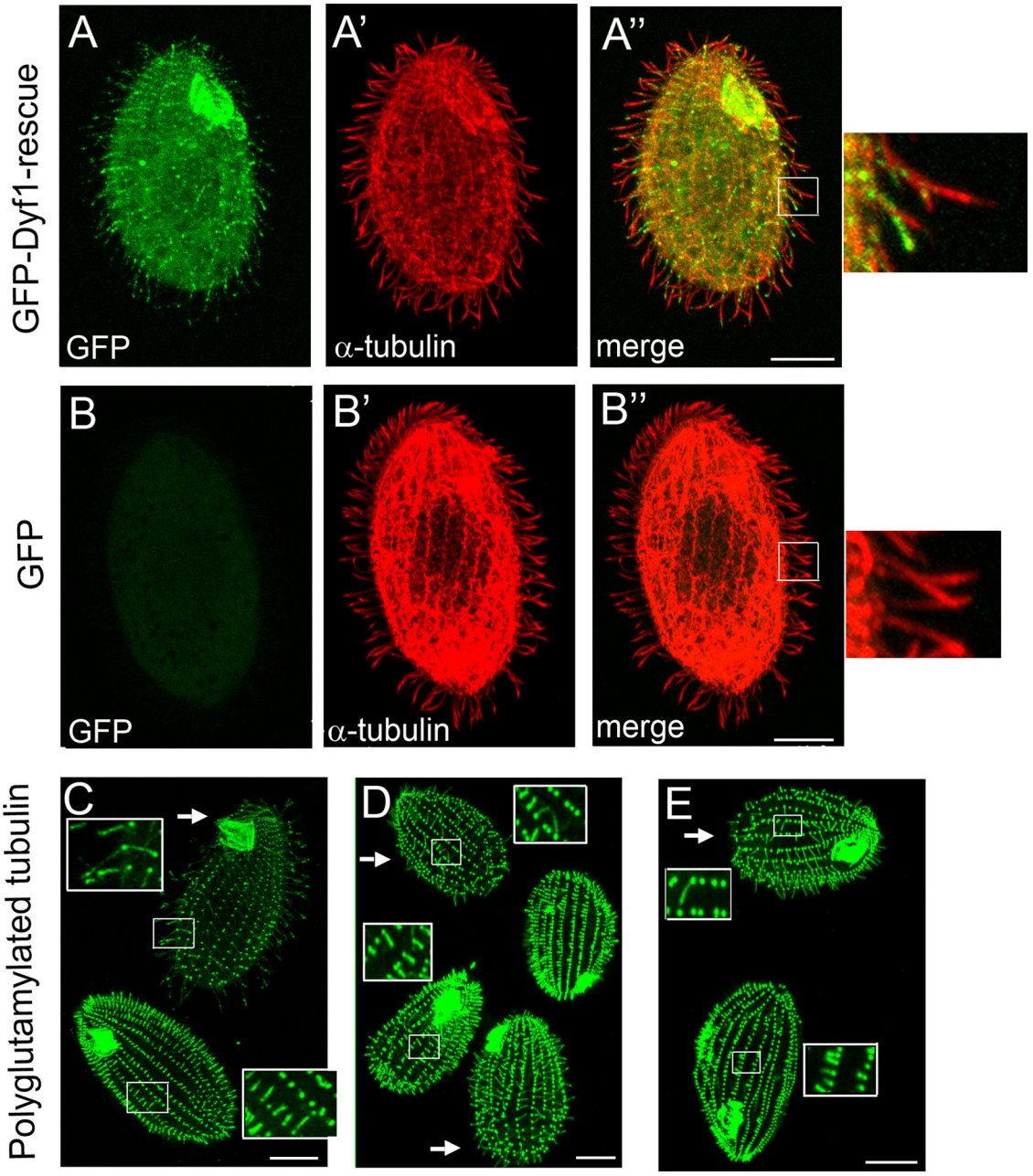


FIG. 5. GFP-DYF1p localizes to axonemes, and basal bodies and axoneme remnants in DYF1Δ cells are hyperglutamylated. (A to B″) GFP distribution in cells expressing GFP-Dyf1p (A to A″) and GFP alone (B to B″). The GFP-DYF1 (A to A″) or GFP (B to B″) transgenes are inserted into the *BTU1* locus, and both operate under the *MTT1* promoter. The GFP-DYF1 transgene was introduced by rescue of DYF1Δ knockout strains, while the GFP transgene was introduced as described previously (65). Cells were induced to express the transgenes by incubation with 2.5 μg/ml $CdCl_2$ for 3 h. On the right are higher magnifications of the boxed areas in panels A″ and B″. (C to E) Growing (C) and cilium-regenerating (30 min) wild-type cells were mixed with either DYF1Δ cells (C and D) or IFT52Δ cells (E) and labeled side by side with the anti-polyglutamylated-tubulin ID5 antibodies. The arrows mark wild-type cells, and the insets show higher magnifications of the boxed areas in panels C to E. Bars, 10 μm.

Dyf1p in an already assembled cilium. The availability of DYF-1 knockout *Tetrahymena* cells will allow systematic mutagenesis of Dyf1p based on functional rescue.

Pathak and colleagues observed a decrease in the levels of tubulin glutamylation in the *dyf-1/fleer* mutant axonemes (40). According to one of their models, DYF-1/fleer acts as a cargo adaptor that links IFT particles to enzymes required for glutamylation of tubulin (40). However, we showed that the residual axonemes in DYF1Δ *Tetrahymena* cells have elevated levels of tubulin polyglutamylation. We also showed that in *Tetrahymena*, an extreme truncation of the axoneme is generally associated with tubulin hyperglutamylation. It is possible that in *Tetrahymena*, in the absence of Dyf1p, tubulin glutamic acid ligase enzymes accumulate in the axoneme remnant. An alternative explanation of the zebrafish DYF-1 knockdown effect on tubulin polyglutamylation can also be considered (40). In the

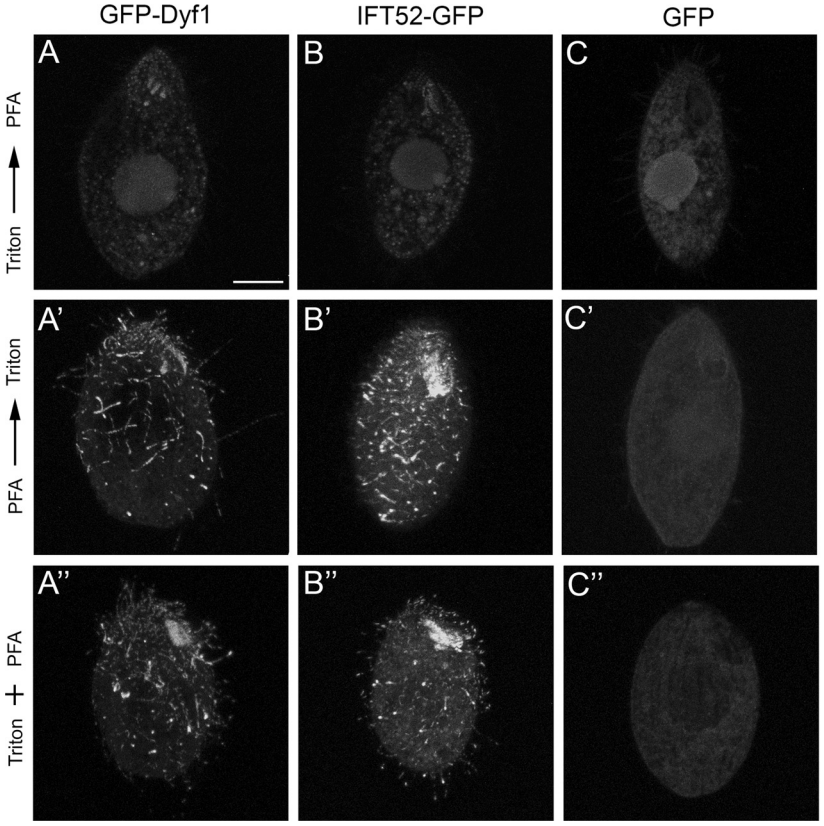


FIG. 6. Dyf1p, like IFT52p, is a component of the detergent-soluble ciliary matrix. Cells expressing GFP-Dyf1p (A, A′, and A″), IFT52p-GFP (B, B′, and B″), and GFP (C, C′, and C″) were fixed using three different methods. The cells shown in panels A to C were permeabilized with Triton X-100 (3 min) and postfixed with paraformaldehyde (PFA). The cells shown in panels A′ to C′ were fixed with PFA and permeabilized with Triton X-100. The cells shown in panels A″ to C″ were simultaneously fixed and permeabilized in a mixture of PFA and Triton X-100. Bar, 10 μm.

axonemes of several organisms, tubulin glutamylation is concentrated on the B tubule of outer doublets (17, 30, 34). If in zebrafish loss of DYF-1 primarily destabilizes the B tubules and the corresponding A tubules remain stable, this in itself could lead to a selective loss of glutamylated tubulin from the axoneme.

In *Tetrahymena*, the consequences of loss of Dyf1p resemble the phenotype of loss of function of anterograde IFT, including deficiencies in the complex B proteins IFT52 (6) and IFT172 (59) and a deficiency in kinesin-2 (7). In contrast, deficiencies in the retrograde IFT do not lead to a loss of the axonemes in *Tetrahymena* (45, 60). These data taken together suggest that Dyf1p is associated with the anterograde IFT. This suggestion is supported by our observations that Dyf1p is present primarily in the detergent-soluble fraction of cilia (Fig. 6). However, in contrast to the anterograde IFT *Tetrahymena* mutants, in DYF1Δ cells the axonemes assemble to some extent. Moreover, some axoneme stubs in DYF1Δ cells have a central pair, while central microtubules fail to assemble in anterograde IFT-deficient cells (6, 7, 33). In fact, the common feature of DYF-1 deficiencies in *C. elegans*, *Tetrahymena*, and zebrafish is that axonemal microtubules in all these models assemble to some extent. Thus, DYF-1 is probably not required for transport of axonemal precursor tubulin. Instead, DYF-1 could serve as an anterograde IFT adapter for cargo that is needed to stabilize the assembling axoneme.

Interestingly, 20% of the basal bodies in *Tetrahymena* DYF1Δ cells lacked an axoneme but had a "bubble" of an apparent ciliary plasma membrane. It is possible that under Dyf1p deficiency the axoneme can initially assemble but breaks down with a delayed resorption of the corresponding ciliary membrane. Alternatively, the ciliary membrane can expand without a corresponding assembly of the axoneme. A similar phenotype was observed for several IFT complex B deficiencies in *Trypanosoma* (1). There is growing evidence that the delivery of precursor membranes destined for cilia is coupled to IFT. For example, multiple proteins that are either components of IFT particles or interact with IFT bind to ciliary membranes or membrane-associated proteins, including Rab8, a small G protein that interacts with the BBSome complex (35), and Elipsa, which interacts directly with IFT20 and indirectly with Rab8 (37). Moreover, IFT20 (an IFT complex B protein) localizes to the Golgi network and is required for targeting polycystin-2 channels to the ciliary membranes (16). Thus, we confirmed earlier observations (1) that during IFT, axoneme assembly and ciliary membrane expansion can be uncoupled under certain conditions.

## ACKNOWLEDGMENTS

This work was supported by National Science Foundation grant MBC-033965 to J.G.

We acknowledge excellent assistance with TEM by Mary Ard (College of Veterinary Medicine, UGA). We thank Winfield Sale (Emory University) for helpful suggestions. We also thank Martin A. Gorovsky (University of Rochester) for SG antibodies, Joseph Frankel (University of Iowa) for the 12G10 antibody (available from the Developmen-

tal Studies Hybridoma Bank), Klaus Weber (Max Planck Institute, Goettingen, Germany) for the ID5 antibody, and Marie-Helene Bré and Nicolette Levilliers (Université Paris-Sud, Orsay, France) for TAP952 and AXO49 antibodies.

## REFERENCES


1. **Absalon, S., T. Blisnick, T. Kohl, G. Toutirais, G. Doré, D. Julkowska, A. Tavenet, and P. Bastin.** 2008. Intraflagellar transport and functional analysis of genes required for flagellum formation in trypanosomes. Mol. Biol. Cell **19:**929–944.
2. **Awan, A., M. Bernstein, T. Hamasaki, and P. Satir.** 2004. Cloning and characterization of Kin5, a novel *Tetrahymena* ciliary kinesin II. Cell Motil. Cytoskeleton **58:**1–9.
3. **Badano, J. L., N. Mitsuma, P. L. Beales, and N. Katsanis.** 2006. The ciliopathies: an emerging class of human genetic disorders. Annu. Rev. Genomics Hum. Genet. **7:**125–148.
4. **Bobinnec, Y., A. Khodjakov, L. M. Mir, C. L. Rieder, B. Eddé, and M. Bornens.** 1998. Centriole disassembly *in vivo* and its effect on centrosome structure and function in vertebrate cells. J. Cell Biol. **143:**1575–1589.
5. **Bré, M. H., V. Redeker, J. Vinh, J. Rossier, and N. Levilliers.** 1998. Tubulin polyglycylation: differential posttranslational modification of dynamic cytoplasmic and stable axonemal microtubules in *Paramecium*. Mol. Biol. Cell **9:**2655–2665.
6. **Brown, J. M., N. A. Fine, G. Pandiyan, R. Thazhath, and J. Gaertig.** 2003. Hypoxia regulates assembly of cilia in suppressors of *Tetrahymena* lacking an intraflagellar transport subunit gene. Mol. Biol. Cell **14:**3192–3207.
7. **Brown, J. M., C. Marsala, R. Kosoy, and J. Gaertig.** 1999. Kinesin-II is preferentially targeted to assembling cilia and is required for ciliogenesis and normal cytokinesis in *Tetrahymena*. Mol. Biol. Cell **10:**3081–3096.
8. **Campbell, P. K., K. G. Waymire, R. L. Heier, C. Sharer, D. E. Day, H. Reimann, J. M. Jaje, G. A. Friedrich, M. Burmeister, T. J. Bartness, L. D. Russell, L. J. Young, M. Zimmer, D. E. Jenne, and G. R. MacGregor.** 2002. Mutation of a novel gene results in abnormal development of spermatid flagella, loss of intermale aggression and reduced body fat in mice. Genetics **162:**307–320.
9. **Cassidy-Hanley, D., J. Bowen, J. Lee, E. S. Cole, L. A. VerPlank, J. Gaertig, M. A. Gorovsky, and P. J. Bruns.** 1997. Germline and somatic transformation of mating *Tetrahymena thermophila* by particle bombardment. Genetics **146:**135–147.
10. **Cole, D. G., D. R. Diener, A. L. Himelblau, P. L. Beech, J. C. Fuster, and J. L. Rosenbaum.** 1998. *Chlamydomonas* kinesin-II-dependent intraflagellar transport (IFT): IFT particles contain proteins required for ciliary assembly in *Caenorhabditis elegans* sensory neurons. J. Cell Biol. **18:**993–1008.
11. **Dentler, W. L.** 1980. Structures linking the tips of ciliary and flagellar microtubules to the membrane. J. Cell Sci. **42:**207–220.
12. **Eddé, B., J. Rossier, J.-P. Le Caer, E. Desbruyères, F. Gros, and P. Denoulet.** 1990. Posttranslational glutamylation of α-tubulin. Science **247:**83–85.
13. **Eisen, J. A., R. S. Coyne, M. Wu, D. Wu, M. Thiagarajan, J. R. Wortman, J. H. Badger, Q. Ren, P. Amedeo, K. M. Jones, L. J. Tallon, A. L. Delcher, S. L. Salzberg, J. C. Silva, B. J. Haas, W. H. Majoros, M. Farzad, J. M. Carlton, R. K. Smith, J. Garg, R. E. Pearlman, K. M. Karrer, L. Sun, G. Manning, N. C. Elde, A. P. Turkewitz, D. J. Asai, D. E. Wilkes, Y. Wang, H. Cai, K. Collins, B. A. Stewart, S. R. Lee, K. Wilamowska, Z. Weinberg, W. L. Ruzzo, D. Wloga, J. Gaertig, J. Frankel, C. C. Tsao, M. A. Gorovsky, P. J. Keeling, R. F. Waller, N. J. Patron, J. M. Cherry, N. A. Stover, C. J. Krieger, C. Del Toro, H. F. Ryder, S. C. Williamson, R. A. Barbeau, E. P. Hamilton, and E. Orias.** 2006. Macronuclear genome sequence of the ciliate *Tetrahymena thermophila*, a model eukaryote. PLoS Biol. **4:**e286.
14. **Evans, J. E., J. J. Snow, A. L. Gunnarson, G. Ou, H. Stahlberg, K. L. McDonald, and J. M. Scholey.** 2006. Functional modulation of IFT kinesins extends the sensory repertoire of ciliated neurons in *Caenorhabditis elegans*. J. Cell Biol. **172:**663–669.
15. **Felsenstein, J.** 1997. An alternating least squares approach to inferring phylogenies from pairwise distances. Syst. Biol. **46:**101–111.
16. **Follit, J. A., R. A. Tuft, K. E. Fogarty, and G. J. Pazour.** 2006. The intraflagellar transport protein IFT20 is associated with the Golgi complex and is required for cilia assembly. Mol. Biol. Cell **17:**3781–3792.
17. **Fouquet, J. P., B. Edde, M. L. Kann, A. Wolff, E. Desbruyeres, and P. Denoulet.** 1994. Differential distribution of glutamylated tubulin during spermatogenesis in mammalian testis. Cell Motil.Cytoskeleton **27:**49–58.
18. **Gaertig, J., M. A. Cruz, J. Bowen, L. Gu, D. G. Pennock, and M. A. Gorovsky.** 1995. Acetylation of lysine 40 in alpha-tubulin is not essential in *Tetrahymena thermophila*. J. Cell Biol. **129:**1301–1310.
19. **Gaertig, J., Y. Gao, T. Tishgarten, T. G. Clark, and H. W. Dickerson.** 1999. Surface display of a parasite antigen in the ciliate *Tetrahymena thermophila*. Nat. Biotechnol. **17:**462–465.
20. **Gaertig, J., and D. Wloga.** 2008. Ciliary tubulin and its post-translational modifications, p. 83–109. *In* B. K. Yoder (ed.), Ciliary function in mammalian development, vol. 85. Elsevier Inc., New York, NY.
21. **Galtier, N., M. Gouy, and C. Gautier.** 1996. SEAVIEW and PHYLO_WIN: two graphic tools for sequence alignment and molecular phylogeny. Comput. Appl. Biosci. **12:**543–548.
22. **Gorovsky, M. A., M.-C. Yao, J. B. Keevert, and G. L. Pleger.** 1975. Isolation of micro- and macronuclei of *Tetrahymena pyriformis*. Methods Cell Biol. **9:**311–327.
23. **Hou, Y., H. Qin, J. A. Follit, G. J. Pazour, J. L. Rosenbaum, and G. B. Witman.** 2007. Functional analysis of an individual IFT protein: IFT46 is required for transport of outer dynein arms into flagella. J. Cell Biol. **176:**653–665.
24. **Inglis, P. N., G. Ou, M. R. Leroux, and J. M. Scholey.** 2007. The sensory cilia of *Caenorhabditis elegans*. WormBook **8:**1–22.
25. **Janke, C., K. Rogowski, D. Wloga, C. Regnard, A. V. Kajava, J.-M. Strub, N. Temurak, J. van Dijk, D. Boucher, A. van Dorsselaer, S. Suryavanshi, J. Gaertig, and B. Eddé.** 2005. Tubulin polyglutamylase enzymes are members of the TTL domain protein family. Science **308:**1758–1762.
26. **Jeanmougin, F., J. D. Thompson, M. Gouy, D. G. Higgins, and T. J. Gibson.** 1998. Multiple sequence alignment with Clustal X. Trends Biochem. Sci. **23:**403–405.
27. **Jerka-Dziadosz, M., I. Strzyzewska-Jowko, U. Wojsa-Lugowska, W. Krawczynska, and A. Krzywicka.** 2001. The dynamics of filamentous structures in the apical band, oral crescent, fission line and the postoral meridional filament in *Tetrahymena thermophila* revealed by the monoclonal antibody 12G9. Protist **152:**53–67.
28. **Kozminski, K. G., P. L. Beech, and J. L. Rosenbaum.** 1995. The *Chlamydomonas* kinesin-like protein FLA10 is involved in motility associated with the flagellar membrane. J. Cell Biol. **131:**1517–1527.
29. **Kozminski, K. G., K. A. Johnson, P. Forscher, and J. L. Rosenbaum.** 1993. A motility in the eukaryotic flagellum unrelated to flagellar beating. Proc. Natl. Acad. Sci. USA **90:**5519–5523.
30. **Lechtreck, K.-F., and S. Geimer.** 2000. Distributon of polyglutamylated tubulin in the flagellar apparatus of green flagellates. Cell Motil. Cytoskeleton. **47:**219–235.
31. **Marshall, W. F., and J. L. Rosenbaum.** 2001. Intraflagellar transport balances continuous turnover of outer doublet microtubules: implications for flagellar length control. J. Cell Biol. **155:**405–414.
32. **Mesland, D. A., J. L. Hoffman, E. Caligor, and U. W. Goodenough.** 1980. Flagellar tip activation stimulated by membrane adhesions in *Chlamydomonas* gametes. J. Cell Biol. **84:**599–617.
33. **Morris, R. L., and J. M. Scholey.** 1997. Heterotrimeric kinesin-II is required for the assembly of motile 9+2 ciliary axonemes on sea urchin embryos. J. Cell Biol. **138:**1009–1022.
34. **Multigner, L., I. Pignot-Paintrand, Y. Saoudi, D. Job, U. Plessmann, M. Rüdiger, and K. Weber.** 1996. The A and B tubules of the outer doublets of sea urchin sperm axonemes are composed of different tubulin variants. Biochemistry **35:**10862–10871.
35. **Nachury, M. V.** 2008. Tandem affinity purification of the BBSome, a critical regulator of Rab8 in ciliogenesis. Methods Enzymol. **439:**501–513.
36. **Nicastro, D., C. Schwartz, J. Pierson, R. Gaudette, M. E. Porter, and J. R. McIntosh.** 2006. The molecular architecture of axonemes revealed by cryoelectron tomography. Science **313:**944–948.
37. **Omori, Y., C. Zhao, A. Saras, S. Mukhopadhyay, W. Kim, T. Furukawa, P. Sengupta, A. Veraksa, and J. Malicki.** 2008. Elipsa is an early determinant of ciliogenesis that links the IFT particle to membrane-associated small GTPase Rab8. Nat. Cell Biol. **10:**437–444.
38. **Orias, E., and L. Rasmussen.** 1976. Dual capacity for nutrient uptake in tetrahymena. IV. Growth without food vacuoles. Exp. Cell Res. **102:**127–137.
39. **Ou, G., O. E. Blacque, J. J. Snow, M. R. Leroux, and J. M. Scholey.** 2005. Functional coordination of intraflagellar transport motors. Nature **436:**583–587.
40. **Pathak, N., T. Obara, S. Mangos, Y. Liu, and I. A. Drummond.** 2007. The zebrafish fleer gene encodes an essential regulator of cilia tubulin polyglutamylation. Mol. Biol. Cell **18:**4353–4364.
41. **Pazour, G. J., B. L. Dickert, and G. B. Witman.** 1999. The DHC1b (DHC2) isoform of cytoplasmic dynein is required for flagellar assembly. J. Cell Biol. **144:**473–481.
42. **Piperno, G., and K. Mead.** 1997. Transport of a novel complex in the cytoplasmic matrix of *Chlamydomonas* flagella. Proc. Natl. Acad. Sci. USA **94:**4457–4462.
43. **Porter, M. E., R. Bower, J. A. Knott, P. Byrd, and W. Dentler.** 1999. Cytoplasmic dynein heavy chain 1b is required for flagellar assembly in *Chlamydomonas*. Mol. Biol. Cell **10:**693–712.
44. **Qin, H., D. T. Burnette, Y. K. Bae, P. Forscher, M. M. Barr, and J. L. Rosenbaum.** 2005. Intraflagellar transport is required for the vectorial movement of TRPV channels in the ciliary membrane. Curr. Biol. **15:**1695–1699.
45. **Rajagopalan, V., A. Subramanian, D. E. Wilkes, D. G. Pennock, and D. J. Asai.** 2009. Dynein-2 affects the regulation of ciliary length but is not required for ciliogenesis in *Tetrahymena thermophila*. Mol. Biol. Cell **20:**708–720.
46. **Redeker, V., N. Levilliers, J.-M. Schmitter, J.-P. Le Caer, J. Rossier, A. Adoutte, and M.-H. Bré.** 1994. Polyglycylation of tubulin: a post-translational modification in axonemal microtubules. Science **266:**1688–1691.
47. **Redeker, V., N. Levilliers, E. Vinolo, J. Rossier, D. Jaillard, D. Burnette, J.**

**Gaertig, and M. H. Bré.** 2005. Mutations of tubulin glycylation sites reveal cross-talk between the C termini of alpha- and beta-tubulin and affect the ciliary matrix in *Tetrahymena*. J. Biol. Chem. **280:**596–606.
48. **Rüdiger, A. H., M. Rüdiger, J. Wehland, and K. Weber.** 1999. Monoclonal antibody ID5: epitope characterization and minimal requirements for the recognition of polyglutamylated alpha- and beta-tubulin. Eur. J. Cell Biol. **78:**15–20.
49. **Sale, W., and P. Satir.** 1976. Splayed *Tetrahymena* cilia. A system for analyzing sliding and axonemal spoke arrangements. J. Cell Biol. **71:**589–605.
50. **Sale, W. S., and P. Satir.** 1977. The termination of the central microtubules from the cilia of *Tetrahymena pyriformis*. Cell Biol. Int. **1:**45–49.
51. **Shang, Y., X. Song, J. Bowen, R. Corstanje, Y. Gao, J. Gaertig, and M. A. Gorovsky.** 2002. A robust inducible-repressible promoter greatly facilitates gene knockouts, conditional expression, and overexpression of homologous and heterologous genes in *Tetrahymena thermophila*. Proc. Natl. Acad. Sci. USA **99:**3734–3739.
52. **Sharma, N., J. Bryant, D. Wloga, R. Donaldson, R. C. Davis, M. Jerka-Dziadosz, and J. Gaertig.** 2007. Katanin regulates dynamics of microtubules and biogenesis of motile cilia. J. Cell Biol. **178:**1065–1079.
53. **Signor, D., K. P. Wedaman, J. T. Orozco, N. D. Dwyer, C. I. Bargmann, L. S. Rose, and J. M. Scholey.** 1999. Role of a class DHC1b dynein in retrograde trasnport of IFT motors and IFT raft particles along cilia but not dentrites, in chemosensory neurons of living *Caenorhabditis elegans*. J. Cell Biol. **147:** 519–530.
54. **Signor, D., K. P. Wedaman, L. S. Rose, and J. M. Scholey.** 1999. Two heteromeric kinesin complexes in chemosensory neurons and sensory cilia of *Caenorhabditis elegans*. Mol. Biol. Cell **10:**345–360.
55. **Smith, E. F., and P. A. Lefebvre.** 1997. PF20 gene product contains WD repeats and localizes to the intermicrotubule bridges in *Chlamydomonas* flagella. Mol. Biol. Cell **8:**455–467.
56. **Snow, J. J., G. Ou, A. L. Gunnarson, M. R. Walker, H. M. Zhou, I. Brust-Mascher, and J. M. Scholey.** 2004. Two anterograde intraflagellar transport motors cooperate to build sensory cilia on *C. elegans* neurons. Nat. Cell Biol. **6:**1109–1113.
57. **Sui, H., and K. H. Downing.** 2006. Molecular architecture of axonemal microtubule doublets revealed by cryo-electron tomography. Nature **442:** 475–478.
58. **Suprenant, K. A., and W. L. Dentler.** 1988. Release of intact microtubule-capping structures from *Tetrahymena* cilia. J. Cell Biol. **107:**2259–2269.
59. **Tsao, C. C., and M. A. Gorovsky.** 2008. Different effects of *Tetrahymena* IFT172 domains on anterograde and retrograde intraflagellar transport. Mol. Biol. Cell **19:**1450–1461.
60. **Tsao, C. C., and M. A. Gorovsky.** 2008. *Tetrahymena* IFT122A is not essential for cilia assembly but plays a role in returning IFT proteins from the ciliary tip to the cell body. J. Cell Sci. **121:**428–436.
61. **Turkewitz, A. P., E. Orias, and G. Kapler.** 2002. Functional genomics: the coming of age for *Tetrahymena thermophila*. Trends Genet. **18:**35–40.
62. **Verhey, K. J., and J. Gaertig.** 2007. The tubulin code. Cell Cycle **6:**2152–2160.
63. **Walther, Z., M. Vashistha, and J. L. Hall.** 1994. The *Chlamydomonas FLA10* gene encodes a novel kinesin-homologous protein. J. Cell Biol. **126:**175–188.
64. **Williams, N. E., C. C. Tsao, J. Bowen, G. L. Hehman, R. J. Williams, and J. Frankel.** 2006. The actin gene ACT1 is required for phagocytosis, motility, and cell separation of *Tetrahymena thermophila*. Eukaryot. Cell **5:**555–567.
65. **Wloga, D., A. Camba, K. Rogowski, G. Manning, M. Jerka-Dziadosz, and J. Gaertig.** 2006. Members of the Nima-related kinase family promote disassembly of cilia by multiple mechanisms Mol. Biol. Cell **17:**2799–2810.
66. **Wloga, D., K. Rogowski, N. Sharma, J. van Dijk, C. Janke, B. Edde, M. H. Bre, N. Levilliers, V. Redeker, J. Duan, M. A. Gorovsky, M. Jerka-Dziadosz, and J. Gaertig.** 2008. Glutamylation on α-tubulin is not essential but affects the assembly and functions of a subset of microtubules in *Tetrahymena*. Eukaryot. Cell **7:**1362–1372.